

Investigation on structural, morphological and optical properties of gold loaded titania nanorods prepared via a novel solvothermal approach

Belina Xavier¹, Mary George², and P. Sagayaraj^{3*}

1 Department of Physics, Stella Maris College, Chennai-600 086, India

2. Department of Chemistry, Stella Maris College, Chennai-600 086, India

3. Department of Physics, Loyola College, Chennai-600 034, India

Abstract

We report a rapid synthesis procedure via solvothermal route for preparing size controlled Au/TiO₂ nanocomposites. Three different Au/TiO₂ nanocomposites are prepared by adjusting the concentration of the precursors and the properties of the products are compared. The formation of nanocomposites is studied by both microscopic and spectroscopic characterization. The UV-Vis absorption spectrum of the prepared samples show the appearance of absorption band due to the surface plasmon resonance of the gold nanoparticles, the observed red shift confirms the formation of Au/TiO₂ nanocomposites. The X-ray diffraction patterns are recorded to confirm the crystal structure of the nanocomposites and to ascertain the presence of Au and TiO₂ nanoparticles. The particle size and the morphology of the nanocomposites are determined by transmission electron microscopy (TEM) and it revealed the presence of spherical Au nanoparticles surrounded by TiO₂ nanorods.

Key words-

composite materials; nanostructures; semiconductors; electron microscopy.

1. Introduction

Nanosized semiconductor particles have been subjected to intense research due to its application in photocatalysis, photovoltaics and electrochromic devices, as well as chemical and biological sensors, largely because of their large band-gap energy, corrosion resistant nature, mechanical durability, and abundant availability and cost effectiveness. Among the various oxide

nanostructured materials, TiO₂ has gained increased attention because of its enhanced properties, cheap fabrication, high specific surface area and pore volume, and wide applications in photocatalysis, gas sensing photoelectrolysis and photovoltaic cells. In several cases, the corrosion or dissolution of the noble metal particles during a photocatalytic reaction becomes problematic in practical applications. Hence, it is necessary to design new strategies to either improve the chemical stability or attain higher photo conversion efficiency. Accordingly, nanocomposites with metal and metal oxide semiconductor become increasingly the strongest candidates as photocatalysts due to their controllable chemical and colloidal stability between metal and metal oxide semiconductors. Photocatalytic efficiency of TiO₂ is greatly enhanced by loading a noble metal (Au). Over the years, many preparation routes have been developed to synthesize gold/TiO₂ nanocomposites. Though there is variety of preparation techniques, the solvothermal method is found to be a simple and cost effective strategy. Until now, this research has been largely focused on synthesis and optical applications. It is generally believed that the solvothermal route offers a straight forward strategy to develop better quality Au/TiO₂ nanocomposites.

Yu et al. synthesized Au/TiO₂ nanocomposites microspheres via a hydrothermal process by employing Tetrabutyl titanate (Ti (OC₄H₉)₄, TBOT) precursor for the synthesis of titania and the Au colloids were obtained using citrate reduction method. The size of the synthesized gold nanoparticles (AuNPs) was around 10 nm, whereas, the size of the titania nanoparticles was in micrometer

range. Li and Zeng hydrothermally synthesized Au@TiO₂ core-shell nanostructure using the TiF₄ precursor for obtaining titania. The AuNPs were synthesized using sodium citrate and the size was found to be 50-100 nm. Baolin et al. developed gold doped TiO₂ nanotubes via a hydrothermal route by using pure anatase TiO₂ nanopowders along with gold colloid. The nanotubes of TiO₂ were in the micrometer range and AuNPs of size around 5 nm were found decorated over the nanotubes of TiO₂. An interesting core-shell Au@TiO₂ nanoparticles with truncated wedge-shaped morphology was reported by Wu et al. with solvothermal approach using TiF₄ precursor for TiO₂ nanoparticles. Gold colloid was prepared using gold chloride and sodium citrate, but the size of the AuNPs could not be controlled to a larger extent. It is inferred that in hydrothermal preparation of Au@TiO₂ composites, the size of Au is controlled to a larger extent, however; as per the available literature a synthetic strategy dealing with good control over the morphology and particle size of TiO₂ is yet to be precisely established while dealing with Au/TiO₂ nanocomposites.

A relatively simple and flexible solvothermal route has been adopted in this work for the formation of Au/TiO₂ nanocomposites. The Au/TiO₂ nanocomposites were prepared with two different concentrations of TiO₂ by a two-step synthesis and the effect of concentration of TiO₂ on the size and properties of Au/TiO₂ nanocomposites are reported. In addition, the ratio of gold and TiO₂ was nearly equalized and the change in the resulting morphology of the gold and TiO₂ nanocomposites is also reported. Preliminary study indicates that among the three samples prepared in this work, the formation of core-shell structured Au@TiO₂ is highly favored when the concentration of the gold and titania was made equal. The striking feature of this investigation lies in the ability to control the size of both gold and titania nanoparticles, especially the size of the titania via a simple solvothermal route.

The as-prepared nanocomposites have been characterized by UV-Vis spectroscopy, Powder X-ray Diffraction analysis (PXRD), Scanning Electron Microscopy (SEM), Energy Dispersive X-ray analysis (EDX) and High Resolution Transmission Electron Microscopy (HRTEM).

2. Experimental Details

2.1. Materials

Hydrogen tetrachloroaurate (I) hydrate (HAuCl₄.H₂O, 99.9%) (Loba Chemi), cetyl trimethylammonium bromide (CTAB, 98%) (Loba Chemi), sodium borohydride (Merck), titanium (IV) isopropoxide (TIPO, 97%) (Aldrich), ethylenediamine tetra-acetic acid (EDTA) (Fisher scientific) and toluene (Merck) were purchased. All chemicals were used as received. Ultra pure water from Millipore was used to prepare the solutions.

2.2. Synthesis

The present synthesis experiment involved the preparation of three samples (GT-A, GT-B and GT-C) by varying the wt% of titania/gold in Au/TiO₂ nanocomposites. The schematic of the preparation of Au/TiO₂ nanocomposites is detailed in Figure 1.

In order to prepare gold nanoparticles, 45 ml of 0.25 mM of HAuCl₄.H₂O aqueous solution was taken and 6.75 x 10⁻³ mol of CTAB powder was added into it. The solution turned light yellow in color. Then, 250 µl of 0.15 M of NaBH₄ was added to the above mixture and the color of solution became brown. The pH was maintained at ~7. This was labeled as solution A. For synthesizing titania, 0.07 g of EDTA was dissolved in 5 ml of water with continuous stirring and then 25 ml of toluene was added. The solution was stirred for 20 minutes and 0.61 ml of Titanium (IV) isopropoxide was then added to the above mixture. Curdy white precipitate was formed. Again, the solution was stirred for 10 minutes. The pH was found to be 7. This solution was labeled as B. Solution A was poured into solution B and stirred for a few minutes. The solution mixture turned into pinkish white color. The above mixture was transferred to a Teflon-lined autoclave and kept for 180 °C for 48 h. The resultant mixture was centrifuged, washed, and the final pinkish white product was dried at 70 °C for 12 h and then collected as sample GT-A. The same procedure was followed to prepare another sample (GT-B) by varying the volume of toluene and TIPO as 37 ml and 0.92 ml respectively. Then for the third sample (GT-C), the concentration of HAuCl₄.H₂O was increased from 0.25 mM to 5 mM and 19 ml of toluene and 0.46 ml of TIPO were used.

2.3. Characterization techniques

The powder X-ray diffraction (PXRD) patterns of the three samples were recorded using RICH SEIFERT X-ray diffractometer (XRD) in 2θ range from 10 to 80° . UV-Vis absorption spectra of the nanopowders were recorded with a VARIAN CARY 5E spectrophotometer at room temperature. For EDX analysis, the samples were deposited onto carbon substrate and loaded into a HITACHI (S-3400N) Scanning Electron Microscope (SEM) equipped with EDAX detector. The as-prepared sample was dispersed in ethanol and sonicated, then placed in the copper grid for HRTEM studies. A JEOL JEM-3010 microscope operated at 200 kV in the bright field mode was used for High-Resolution Transmission Electron Microscopy (HRTEM).

2.4 Results and Discussion

In the present work, AuNPs were prepared using a simple one-step non seeded approach. The formation of AuNPs is instantaneous upon addition of the reducing agent. On the other hand, for forming of titania, titanium isopropoxide is used as a precursor, which is highly reactive with water. TIPO is comparatively easier to handle than TiF_4 or TBOT. The precipitation was done using Ti-EDTA complex, resulting in a controlled hydrolysis. This could be attributed to the fact that EDTA being a highly polar medium, ultimately influences the non-polar medium of toluene to get polarized and thus encouraging controlled hydrolysis.

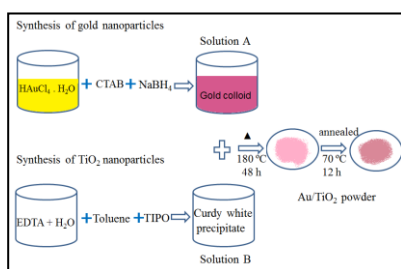


Fig. 1. Schematic representation of solvothermal synthesis of Au/TiO₂ nanocomposites

Figure 2 shows the UV-Vis absorption spectra of pure gold nanoparticle (for comparison) along with the three samples of Au/TiO₂ nanocomposites. For pure AuNPs, the absorption band is seen at 523 nm. The UV-Vis absorption spectra of GT-A, GT-B

and GT-C nanocomposites confirm the appearance of absorption bands at 547 nm, 545 nm and 543 nm respectively, which could be attributed to the surface plasmon resonance (SPR) response of gold. It is further evident that there is a red shift in the peak position corresponding to all the three samples (GT-A, GT-B and GT-C) with respect to the pure AuNPs. The observed red shift in plasmon resonance is attributed to the dielectric constant of the surrounding matrix upon encapsulation. It is clear that the red shift is related to the presence of TiO₂ in the system. Marzan et al. attributed the red shift in the peak position of gold colloids to the increase in medium refractive index. The TiO₂ refractive index is larger than that of water, which causes a red shift in the surface plasmon absorption band of gold.

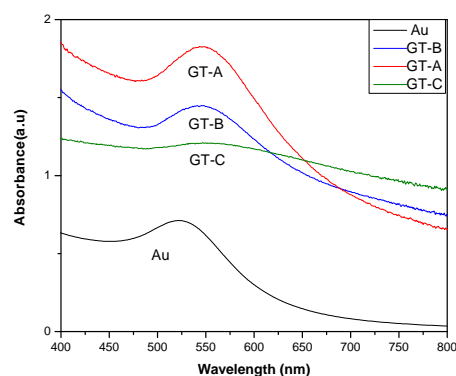


Fig. 2. UV-Vis absorption spectra of pure gold nanoparticle GT-A, GT-B and GT-C

The morphology of the samples was analyzed by SEM. From the SEM images (Figure 3), it is confirmed that the size of the aggregates of the hybrid materials decreases with increase in concentration of TIPO solution. The images also show the presence of TiO₂ heterogenous layers coated with AuNPs and the coating is neatly uniform.

The energy dispersive X-ray analysis (EDX) of Au/TiO₂ nanocomposites (Figure 4) indicates the presence of only the gold and TiO₂ components. The result suggests that all the samples prepared in the present synthesis procedure exhibit high purity without the trace of any kind of impurity. EDX spectra of the three samples indicate that wt% gold is 0.96, 3.31 and 9.28 for GT-A, GT-B and GT-C nanocomposites respectively.

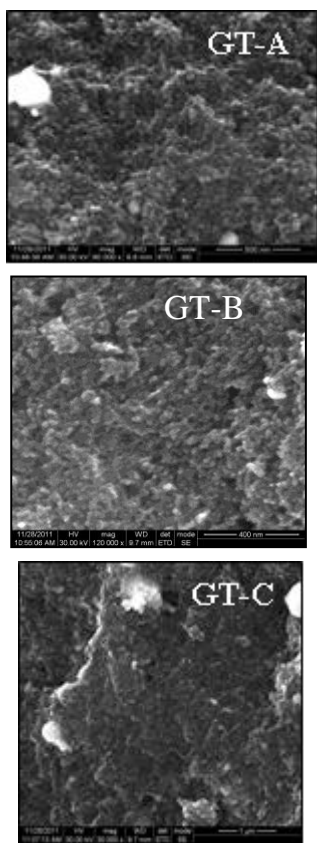


Fig. 3. SEM images of GT-A, GT-B and GT-C

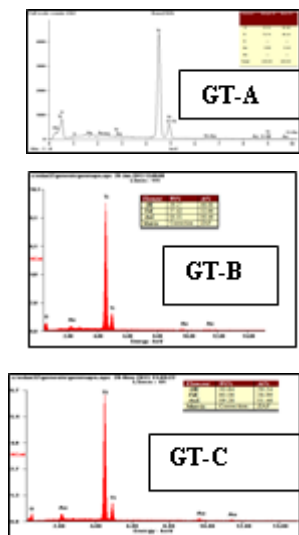


Fig. 4. EDX patterns of GT-A, GT-B and GT-C

The powder X-ray diffraction patterns (Figure 5) of GT-A, GT-B and GT-C nanocomposites confirm the presence of both TiO₂ and gold nanoparticle. The peaks are indexed for both gold and titania. The presence of gold is evident by the peaks

representing the (1 1 1), (2 0 0) and (2 2 0) planes. PXRD data confirms that TiO₂ is tetragonal with body centered lattice and belongs to the anatase phase. The AuNPs are found to be cubic with face centered crystal lattice. This confirms the formation of nanocomposites of TiO₂ and gold. The observed patterns also reveals that the TiO₂ layers are formed on the surface of face centered cubic (fcc) metallic Au nanocrystals (JCPDS No. 01-1174) after 48 h under solvothermal conditions and have anatase-type crystalline phase (JCPDS No. 21-1272) without amorphous or additional phases. It is evident from the diffractogram for the GT-C nanocomposites that the peaks due to gold are more prominent and strong in comparison to the GT-A and GT-B samples. This is due to the increased presence of gold in this sample, which was achieved by increasing the wt% of gold in the sample.

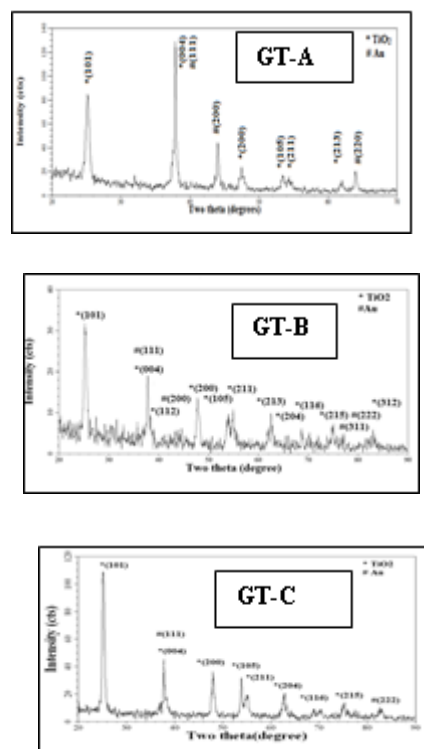


Fig. 5. Powder X-ray diffraction patterns of GT-A, GT-B and GT-C

It is evident that the particle size of both gold and titania in the third sample (GT-C) is controlled to a greater extent when compared to the first two samples. In Au/TiO₂ nanocomposites, the gold particle size is a key

factor that could significantly influence their catalytic efficiencies. It is well known that small AuNPs with diameter less than 5 nm usually show high catalytic activities. However, recently Murdoch et al. found that the Au/TiO₂ hybrids exhibited increasing hydrogen production rate as the loading Au particle size increases up to 12 nm. The particle size of gold nanoparticle in the composite is around 8-10 nm which reveals that the Au/TiO₂ nanocomposites is likely to show more effective photocatalytic activity.

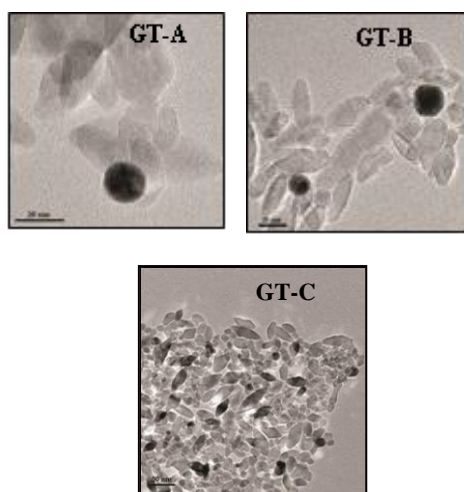


Fig. 6. TEM images of (a) GT-A (b) GT-B and (c) GT-C

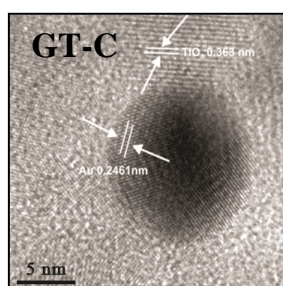


Fig. 7. HRTEM image of GT-C

The TEM images recorded for GT-A, GT-B and GT-C samples are shown in Figure 6. It clearly demonstrates that each one of these nanocomposites have a varying level of Au coating and morphology. The TEM image (Figure 6a) of GT-A nanocomposites reveals

the formation of both gold and TiO₂ nanoparticles. TiO₂ layers are grown on one side of the spherical gold particles. Whereas in Figure 6b (for GT-B), the AuNPs are seen surrounded by the TiO₂ nanorods, indicating the formation of heterogeneous TiO₂ layers on AuNPs. It is clear that the TiO₂ layers have grown densely around the spherical gold particles. The size of the AuNPs is around 10 nm for both GT-A and GT-B samples and the diameter of the titania nanorods is around 20 nm and 15 nm for GT-A and GT-B respectively. Among the three samples, GT-C (Figure 6c) exhibits an interesting scenario, where one could find a high level of Au deposition over TiO₂ nanorods. These nanorods are found to be nearly monodisperse with a low level of agglomeration. The size of the gold nanoparticle in GT-C is around 8 nm and the observed diameter of the titania nanorod is around 10-13 nm. The aspect ratio of TiO₂ nanorods for GT-A, GT-B and GT-C nanocomposites is found to be 2.0, 2.66 and 3.33 respectively. It is confirmed from the TEM analysis that among the three samples control over the size and morphology is best achieved in GT-C. From Figure 6c, it is further evident that in sample GT-C, with its slightly higher wt% of gold, the Au/TiO₂ nanocomposites shows increased presence of nearly core-shell structures. In contrast to the earlier works carried out by Wu et al. and Hajiesmaeilbaigi et al., the size of both gold nanoparticle and titania is controlled to a larger extent and also improved AuNPs coating over the TiO₂ nanorods has been achieved in this work by optimizing the concentration of gold and TiO₂.

To study the morphology of Au/TiO₂ nanocomposites deeply, HRTEM of the sample was taken. Figure 7 depicts the HRTEM image of the Au/TiO₂ nanocomposites (GT-C) which reveals the well-defined interface and continuity between metallic Au nanoparticles and the TiO₂ layer. This is indicative of the strong interaction between the exposed Au atoms and -O-Ti-O-bonds in TiO₂ crystals. The spacing between the adjacent lattice fringes is 0.2461 nm for the Au and 0.363 nm for TiO₂, which is close to the d-spacing of the (111) plane of fcc metallic Au ($d = 0.235$ nm; JCPDS No. 01-1174) and anatase-type TiO₂ ($d = 0.352$ nm; JCPDS No.

21-1272), revealing that the epitaxial formation of (101) crystal planes of TiO₂ near the Au-TiO₂ interface due to matching with exposed Au (111) planes keeps the interfacial energy low. Kang et al. demonstrated an improvement in the electron transport of a photoelectrode based on smaller nanorods (4 nm × 20 nm). Hence by properly tuning the size and the shape of nanoparticles, it is possible to fabricate photo electrodes responding to both requirements of large surface area and efficient electron transfer.

4. Conclusion

The present investigation demonstrated the formation of Au/TiO₂ nanocomposites via a cost effective and straight forward solvothermal approach. The experiments confirmed the high yield and reproducibility of the sample. Control over the sizes of the AuNPs and as well as titania nanorods was achieved with appropriate choice of precursors, solvent, complexing agent and temperature. The UV-Vis absorption spectra of the Au/TiO₂ nanocomposites show considerable red shift in wavelength when compared to pure gold and thus ascertained the formation of the Au/TiO₂ nanocomposites. Best results are obtained when the concentration ratio of the Au/TiO₂ precursors was made nearly equal. A nearly core-shell structure is evident from HRTEM image. The ability to fine-tune the size, morphology and the level of coating in Au/TiO₂ nanocomposites is likely to encourage new kinds of applications in emerging areas of research.

References

1. M. Kitano, K. Tsujimaru, M. Anpo, *Top. Catal.* 49 (2008) 4-17.
2. A. Solanki, J.D. Kim, K.B. Lee, *Nanomedicine.* 3 (2008) 567-578.
3. J. Yu, G. Dai, B. Huang, *J. Phys. Chem. C* 113 (2009) 16394-16401.
4. P.V. Kamat, *J. Phys. Chem. C* 111 (2007) 2834-2860.
5. V. Subramanian, E. Wolf, P.V. Kamat, *J. Phys. Chem. B* 105 (2001) 11439-11446.
6. W.J. Wang, J.L. Zhang, F. Chen, D.N. He, M. Anpo, *J. Colloid Interface Sci.* 323 (2008) 182-186.
7. R.T. Tom, A.S. Nair, N. Singh, M. Aslam, C.L. Nagendra, R. Philip, K. Vijayamohan, T. Pradeep, *Langmuir* 19 (2003) 3439-3445.
8. Pastoriza-Santos, D.S. Koktysh, A.A. Mamedov, M. Giersig, N.A. Koto, L.M. Liz Marzan, *Langmuir* 16 (2000) 2731-2735.
9. J. Li, H.C. Zeng, *Angew. Chem. Int. Ed.* 44 (2005) 4342-4345.
10. X.F. Wu, H.Y. Song, J.M. Yoon, Y.T. Yu, Y.F. Chen, *Langmuir* 25 (2009) 6438-6447.
11. Z. Baolin, S. Zhenming, C. Xiao, W. Shurong, Z. Shoumin, W. Shihua, H. Weiping, *Chinese Sci. Bull.* 50 (2005) 7711-7713.
12. L. M. Liz Marzan, M. Giersig, P. Mulvaney, *Langmuir* 12 (1996) 4329-4335.
13. M. Haruta, *Catal. Today* 36 (1997) 153-166.
14. M. Valden, X. Lai, D.W. Goodman, *Science* 281 (1998) 1647-1650.
15. M. Murdoch, G.I.N. Waterhouse, M.A. Nadeem, J.B. Metson, M.A. Keane, R.F. Howe, J. Llorca, H. Idriss, *Nat. Chem.* 3 (2011) 489-492.
16. F. Hajiesmaeilbaigi, A. Motamedi, M. Ruzbehani, *Laser Physics* 20 (2010) 508-511.
17. Y.H. Zheng, L.R. Zheng, Y.Y. Zhan, X.Y. Lin, Q. Zheng, K.M. Wei, *Inorg. Chem.* 46 (2007) 6980-6986.
18. R. Buonsanti, V. Grillo, E. Carlino, C. Giannini, M.L. Curri, C. Innocenti, C. Sangregorio, K. Achterhold, F.G. Parak, A. Agostiano, P.D. Cozzoli, *J. Am. Chem. Soc.* 128 (2006) 16953-16970.
19. S.H. Kang, S.H. Choi, M.S. Kang, J.Y. Kim, H.S. Kim, T. Hyeon, Y.E. Sung, *Adv. Mater.* 20 (2007) 54-58.